

T. Kitamura for Plat-E cells and pMXs retroviral vectors, and R. Farese for RF8 ES cells. This study was supported in part by a grant from the Program for Promotion of Fundamental Studies in Health Sciences of National Institute of Biomedical Innovation (NIBIO), a grant from the Leading Project of Ministry of Education, Culture, Sports, Science, and Technology (MEXT), a grant from Uehara Memorial Foundation, and grants-in-aid for scientific research of

Japan Society for the Promotion of Science (JSPS) and MEXT (to S.Y.). K.O. was a JSPS research fellow. H.H. is supported by a Japanese government (MEXT) scholarship. The authors are filing a patent based on the results reported in this paper.

Supporting Online Material
www.sciencemag.org/cgi/content/full/1164270/DC1
Materials and Methods

Figs. S1 to S6
Tables S1 and S2

6 August 2008; accepted 25 September 2008
Published online 9 October 2008;
10.1126/science.1164270
Include this information when citing this paper.

Insights into Translational Termination from the Structure of RF2 Bound to the Ribosome

Albert Weixlbaumer,* Hong Jin,* Cajetan Neubauer, Rebecca M. Voorhees, Sabine Petry,† Ann C. Kelley, Venki Ramakrishnan‡

The termination of protein synthesis occurs through the specific recognition of a stop codon in the A site of the ribosome by a release factor (RF), which then catalyzes the hydrolysis of the nascent protein chain from the P-site transfer RNA. Here we present, at a resolution of 3.5 angstroms, the crystal structure of RF2 in complex with its cognate UGA stop codon in the 70S ribosome. The structure provides insight into how RF2 specifically recognizes the stop codon; it also suggests a model for the role of a universally conserved GGQ motif in the catalysis of peptide release.

In nearly all species, three stop codons, UGA, UAG, and UAA, signal the end of the coding sequence in mRNA. These stop codons are decoded by a protein factor termed a class I release factor (RF) (1, 2). In bacteria, there are two such factors with overlapping specificity: RF1 recognizes UAG, RF2 recognizes UGA, and both recognize UAA. In eukaryotes, a single RF, eRF1, recognizes all three stop codons. The mechanism by which RFs specifically decode stop codons and catalyze peptidyl-tRNA hydrolysis is a fundamental problem in understanding translation.

Elements of RFs involved in catalysis and stop-codon recognition have been proposed, using sequence analysis combined with biochemistry and genetics. A universally conserved tripeptide sequence, GGQ (3), has been implicated in the hydrolysis of the peptide chain from tRNA (4). Exchanging a tripeptide motif between RF1 and RF2 [P(A/V)T in RF1; SPF in RF2] switches their respective specificities for UAG and UGA

and catalyzes the hydrolysis of the peptide chain from tRNA (4). Exchanging a tripeptide motif between RF1 and RF2 [P(A/V)T in RF1; SPF in RF2] switches their respective specificities for UAG and UGA

(5). Hydroxyl-radical probing suggested that the SPF and GGQ motifs were close to the decoding center and peptidyl transferase center (PTC), respectively (6).

The structure of the eukaryotic eRF1 suggested that the distance between its codon-recognition and GGQ motifs was compatible with the approximately 75 Å distance between the decoding center and the PTC (7). However, eRF1 has no sequence or structural homology to bacterial RFs. The crystal structure of a bacterial RF2 (8) showed that the distance between the SPF and GGQ motifs was about 23 Å and thus incompatible with their simultaneous involvement in decoding and peptide release. This anomaly was resolved when low-resolution structures (9–11) showed that the conformation of RF2 when bound to the ribosome was different, so that the GGQ and SPF/PVT motifs were localized to the PTC and decoding center, respectively. However, the resolution of these

Medical Research Council (MRC) Laboratory of Molecular Biology, Hills Road, Cambridge CB2 0QH, UK.

*These authors contributed equally to this work.

†Present address: Department of Cellular and Molecular Pharmacology, University of California, San Francisco, 600 16th Street, San Francisco, CA 94158-2517, USA.

‡To whom correspondence should be addressed. E-mail: ramak@mrc-lmb.cam.ac.uk

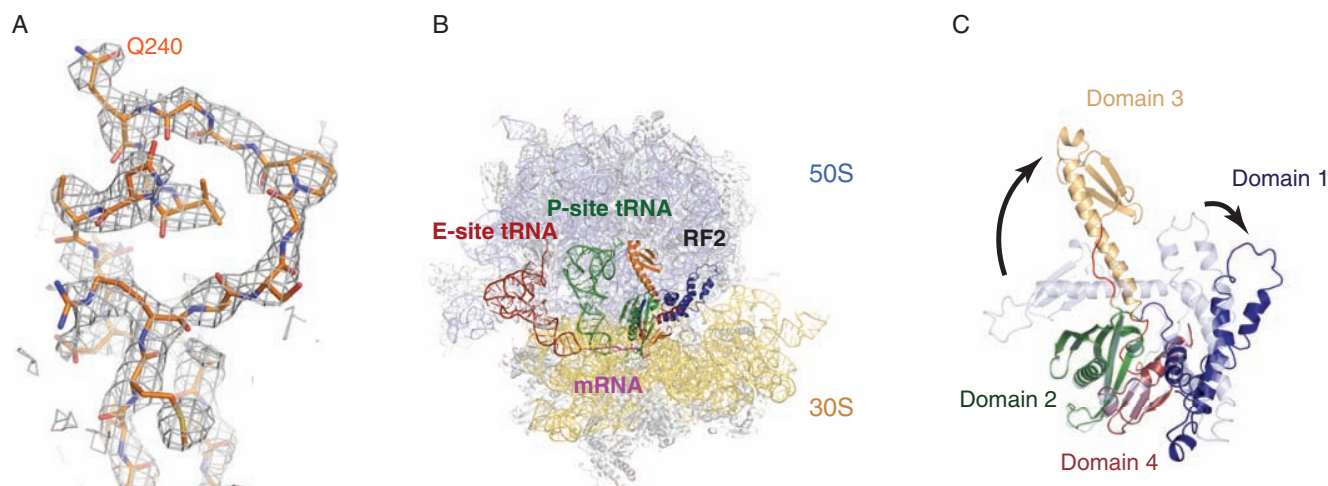


Fig. 1. The structure of RF2 in the ribosome. **(A)** Unbiased difference Fourier maps showing the density of RF2 in the peptidyl transferase center of the ribosome. **(B)** Overview of the structure showing the 50S subunit (light blue), the 30S subunit (yellow) with E-site tRNA (red), P-site tRNA (green), and RF2 colored by domains as in **(C)**. The mRNA is shown in magenta. **(C)** Conformational differences between the isolated crystal structure of RF2 (15) (shown in light blue), and the ribosome-bound form (colored by domains as labeled) are indicated. Loop regions connecting domain 3 with domains 2 and 4, that undergo substantial conformational changes, are highlighted in red.

structures was too low to reveal detailed interactions of RFs with the ribosome.

Two years ago, our laboratory identified a crystal form of the *Thermus thermophilus* ri-

bosome that diffracts to high resolution in the presence of both A- and P-site ligands (12), thus providing a way out of this impasse. Using this crystal form, we report a structure, refined to a

resolution of 3.45 Å, of RF2 bound to a 70S ribosome containing the RF2-specific UGA stop codon (whose nucleotides are named U1, G2, and A3) in the A site (13). The structure shows details of stop-codon recognition by RF2 as well as interactions of RF2 with the PTC and other regions of the ribosome, including helix 69 (H69) and the L11 region. This crystal form was also used in a recent structure of RF1 bound to the ribosome containing a UAA codon (14).

Initial refinement of the data by using a model of the empty ribosome showed clear difference density for the bound ligands (Fig. 1A). A complete model for the ribosome in complex with P- and E-site tRNA^{Phe}, mRNA, and RF2 was thus built and refined (13) (Fig. 1B). Compared with the crystal structure of isolated *T. thermophilus* RF2 (15), the factor in complex with the ribosome underwent major conformational changes. As expected from earlier low-resolution studies (9–11), domain 3 of RF2 peeled away from domains 2 and 4 (15) (Fig. 1C), placing the GGQ motif in the PTC, whereas domains 2 and 4 interact with the decoding center. Domain 1 shifted slightly and interacts with the L11 region of the 50S subunit (see fig. S1 for details). These global conformational changes were accompanied by rearrangements of specific regions (Fig. 1C).

At the decoding center, RF2 induces changes that are markedly different from those induced by paromomycin or tRNA binding to sense codons (16, 17) (Fig. 2A). In standard decoding, three conserved nucleotides in the 30S ribosomal subunit, A1492, A1493, and G530 (*Escherichia coli* numbering is used throughout), change conformation upon tRNA binding and closely interact with the minor groove of the codon-anticodon helix. These conformational changes would clash with RF2, explaining why paromomycin promotes tRNA binding but abolishes RF binding (18). In its new orientation, A1493 stacks

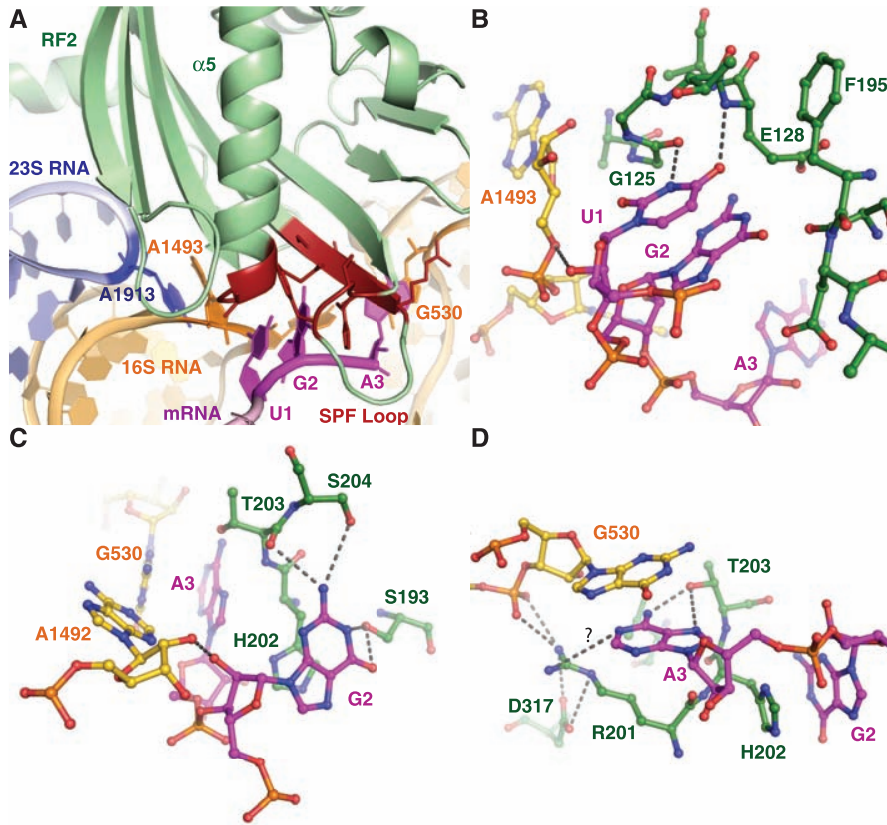


Fig. 2. Interaction of RF2 with the stop codon in the decoding center. (A) Overview of the decoding center, showing the UGA stop codon (magenta). Domain 2 of RF2 is shown in green, except for parts interacting with the codon, which are shown in red. Key bases from 16S RNA and A1913 of 23S RNA are also shown. (B to D) Details of interactions at the first (B), second (C), and third (D) positions of the stop codon with elements of RF2 and the decoding center.

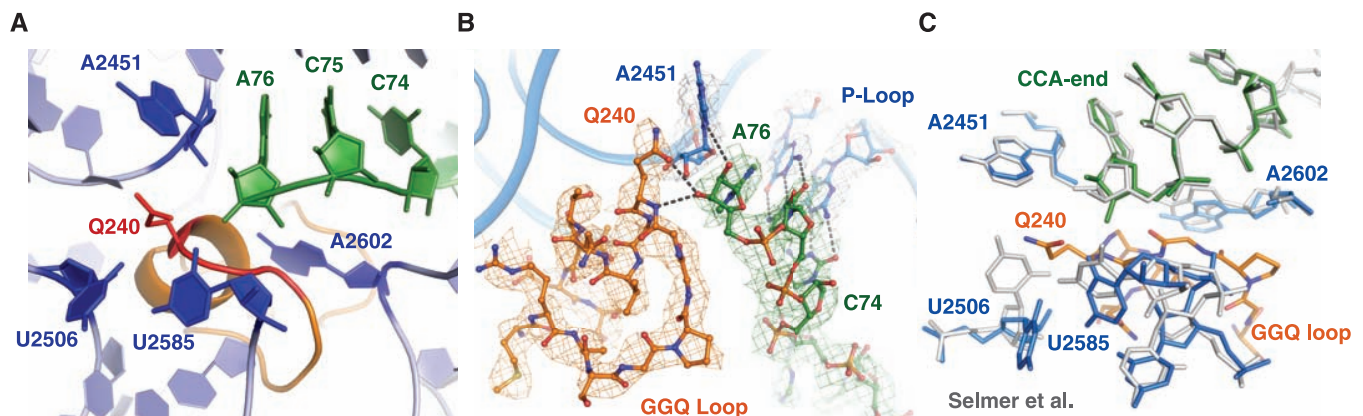


Fig. 3. Interaction of RF2 with the peptidyl transferase center showing the terminal CCA of P-site tRNA (green), the conserved GGQ motif of RF2 (red), and key bases of 23S RNA (blue). (B) Interaction of the GGQ loop of RF2 (orange) with the terminal ribose of P-site tRNA (green), showing σ_A weighted $3mF_{obs} - 2DF_{calc}$ maps, where m is the figure of merit, D is the σ_A weight, and F_{obs} and F_{calc} are the

observed and calculated structure factors, respectively. Potential hydrogen bonds between the conserved Q240 and the ribose of P-site tRNA are shown. (C) Changes in the peptidyl transferase center upon RF2 binding compared with the 70S structure with an empty A site (gray) (12). The structure shows that RF2 would clash with elements of 23S RNA and induces conformational changes, in particular in U2506 and U2585.

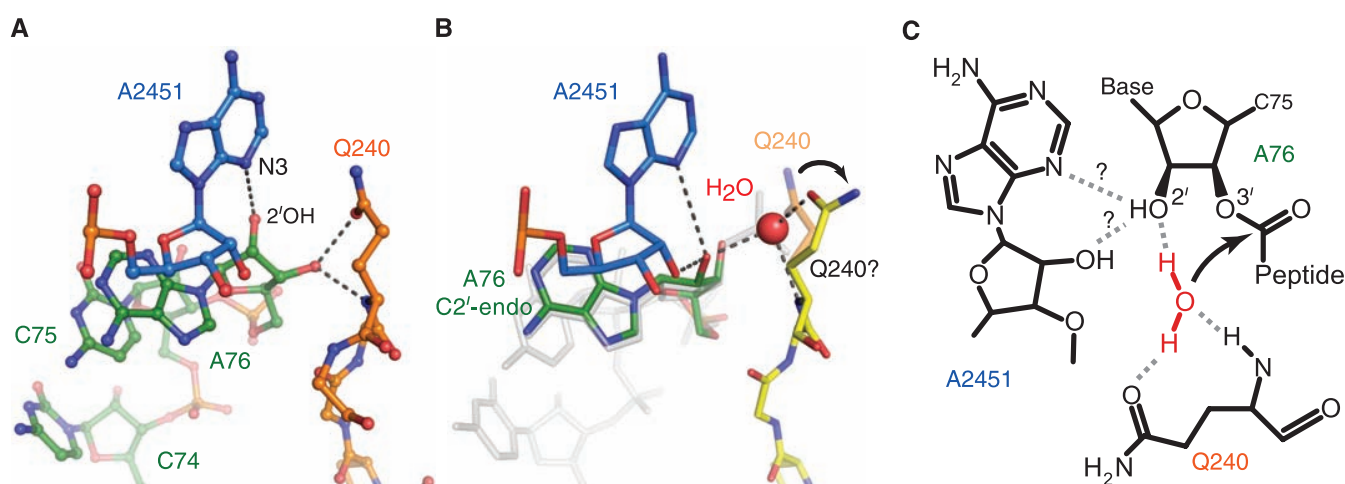


Fig. 4. A model of the substrate complex that suggests the basis for catalysis. **(A)** The interaction of Q240 of RF2 and A2451 of 23S RNA in the current structure. **(B)** A proposed structure showing how a minor change in the orientation of Q240 would allow it to coordinate a water molecule (transparent orange versus yellow). In gray is a transition-state analog superposed on this structure [1VQ7, taken from (24)] that was

used to place the putative water that would take part in a nucleophilic attack on the ester bond. **(C)** A schematic representation of how a network of interactions among the conserved Q240, the coordinated water molecule that is the attacking nucleophile, the ribose of A76 of P-site tRNA (in C2'-endo conformation), and A2451 would act to facilitate catalysis.

on A1913 of 23S RNA, which probably plays a role in signal transduction from the decoding center to the PTC.

The structure sheds light on the basis of stop-codon recognition by RF2. At the first position, two conserved glycines at the tip of helix $\alpha 5$ in domain 2 make important backbone contacts with U1 of the stop codon (Fig. 2B). A purine at this position would result in a steric clash with the backbone of both G125 and G126. The N3 of U1 can make a hydrogen bond with the carbonyl group of G125, and the O4 is within hydrogen-bonding distance of the backbone amide of E128. These interactions would not occur with a C. Together with the recent structure of RF1 bound to the ribosome (14), these observations explain why U is required at the first position of all stop codons.

Only the first amino acid in the SPF motif directly interacts with the second base of the stop codon, via hydrogen bonds between S193 and the O6 and N1 of G2 (Fig. 2C). Similar interactions with the hydroxyl group of S193 would be possible with the N6 and N1 of A, which suggests why an A would also be recognized at this position. The imidazole ring of H202 makes a stacking interaction with the second base. Though a pyrimidine would stack with H202 in a similar fashion, complete desolvation of the Watson-Crick edge would be required without the formation of compensatory hydrogen bonds. Additional conserved elements are important for stop-codon recognition: both the hydroxyl of S204 and the carbonyl backbone of T203 can make hydrogen bonds with the N2 of G2.

Discrimination at the third position appears to be more complex. Although both RFs recognize an A at this position, RF2 miscodes a UGG codon with an error rate of 1 out of 2400, which is almost an order of magnitude worse than it miscodes UGU or UGC (19). The third base A3

does not stack on G2 but instead on G530 of 16S RNA (Fig. 2D). This stacking interaction would be far less favorable for a pyrimidine, which explains the discrimination against U or C at this position. The hydroxyl group of T203 can donate a proton to the N7 of A3 and accept one from its N6. With a G, similar hydrogen bonds could not be formed simultaneously to both its O6 and N7. However, T203 is also present in RF1, which can accept a G at the third position, suggesting that other interactions monitor this position. The terminal amino group of R201, which is conserved in RF2 but absent in RF1, is within hydrogen-bonding distance of the phosphate of U531 and D317 in domain 4 of RF2. These interactions could position the arginine to act as a hydrogen-bond donor for the N1 of A3, which would not be possible with a G. However, the arginine is poorly ordered in the structure.

The structure thus provides a rationale for the specific recognition of UAA and UGA by RF2 and, in conjunction with the recent structure of RF1, clarifies many of the elements involved in stop-codon recognition. However, it is clear that the tripeptide motif identified genetically (5) is only partially responsible for recognition. Other residues, some of which have been discussed, are probably involved in conferring specificity. Moreover, mutations in RF2 distant from the codon give rise to bacterial RFs with altered specificity (20). This suggests that recognition and miscoding by RFs are more complex and may involve the kind of tradeoff between binding energy and induced conformational changes that has been observed for tRNA recognition (21). The observation that the accuracy of termination arises from both a binding component and a catalytic rate component (19) is also fully consistent with the idea that codon recognition by RFs is followed by induced structural rearrangements that lead to catalysis.

The GGQ motif essential for catalysis is positioned in the heart of the PTC (Fig. 3A). The loop within domain 3 that contains this conserved tripeptide shifts considerably when bound to the ribosome as compared with the isolated crystal structure (15). In the modeled loop, both glycines adopt a backbone conformation disallowed for any other amino acid, which explains their universal conservation and the drastic reduction in *in vitro* RF activity upon their mutation (22, 23). The glutamine side chain Q240 was modeled and refined in an orientation that is consistent with the initial unbiased difference Fourier maps (Fig. 1A), which places its side-chain carbonyl within hydrogen-bonding distance of the ribose of A76 of P-site tRNA (Fig. 3B). After refinement, difference Fourier maps also suggest the existence of a second conformation similar to that in the recent structure of RF1 bound to the ribosome, where it is pointed away from the ribose (14). The resolution is not high enough to distinguish between the C2'- and C3'-endo conformations of the ribose. In Fig. 3B, the ribose was modeled in a C3'-endo conformation, which in addition to a bond between the glutamine oxygen to the 3'-OH of A76 also allows a bond between the backbone amide of Q240 and the 3'-OH of A76. This backbone interaction was observed with RF1 (14), where it has been suggested to be important for product stabilization. The alternative C2'-endo conformation seen in other structures (12, 24) would still allow the glutamine side-chain oxygen to make hydrogen bond with the 2'-OH of A76 but would preclude formation of a hydrogen bond with the main-chain amide.

RF2 also induces changes in the PTC as compared with the structure of the ribosome with an empty 50S A site (12). The GGQ loop would clash with U2506 and U2585 if they remained in

the same conformation as when the A site is unoccupied. Thus, both residues have moved as a result of RF2 binding (Fig. 3C). As suggested previously (24), the movement of U2585 away from the ester bond of peptidyl tRNA opens the bond to nucleophilic attack by water, whereas in the uninduced state it would be protected by U2585 in the absence of an A-site ligand. The changes induced by the binding of the GGQ loop that expose the ester bond to nucleophilic attack must be a major component of the catalytic mechanism of RFs and, as suggested previously, show how similar changes induced by deacylated tRNA binding can catalyze peptide release (24).

The glutamine side chain was proposed to directly coordinate a water molecule during hydrolysis of the peptidyl-tRNA ester bond (7). Its mutation had a less drastic effect on activity than mutating either glycine (22, 23); however, the rate enhancement due to the glutamine must nevertheless be important because it is universally conserved, and RFs containing a glutamine mutation fail to complement defective RFs in vivo (25).

The structure, which is of the state after peptide release (Fig. 4A), makes it possible to propose a model for catalysis that rationalizes the available biochemical data by using substrate and transition-state analog structures. The superposition of a transition-state analog of peptidyl transfer from a 50S subunit complex (24) shows that only a small change in the dihedral angles of the conserved Q240 would be sufficient to accommodate a water molecule positioned for nucleophilic attack on the peptidyl-tRNA ester bond (Fig. 4B). As in models presented earlier (7, 26), the side-chain oxygen of Q240 could be involved in hydrogen bonding with a water molecule (Fig. 4C). The glutamine is normally methylated in vivo, and the methylation is known to stimulate termination (27). Presumably, the methylation would help direct the amine away from the ribose, thus positioning the oxygen for coordination with the water molecule. By acting as a hydrogen bond donor to N3 of A2451 (or its 2'-OH), the 2'-OH of A76 (modeled in the C2'-endo conformation, as seen in previous studies) is positioned to accept the second hydrogen of the attacking water, positioning the water oxygen for inline attack on the ester. Our proposed model also explains the minimal effect of A2451 mutants on peptide release (28) because all four bases contain a hydrogen-bond acceptor in the position of the N3 of A2451 and have a 2'-OH. Furthermore, the involvement of the 2'-OH of A76 agrees with data showing a substantial effect on the peptide hydrolysis of a 2'-deoxyadenosine mutant at this position (29). The specific coordination of a water by glutamine is consistent with studies showing that alternative nucleophiles are not affected by its mutation (23). A recent molecular-dynamics study also proposes that the glutamine oxygen directly coordinates a water molecule, and suggests that mutation to alanine allows a second water molecule to compensate for the glutamine oxygen (26). Finally,

the mechanism and the involvement of the 2'-OH of the peptidyl tRNA have similarities with the peptidyl transferase reaction (23).

Mutations of A2602 were observed to reduce the rate of peptide release (28), but other experiments reported that an abasic 2602 had no effect on the reaction rate (30). The structure shows that a direct involvement of A2602 in catalysis can be excluded, but it is possible that the nucleotide is involved in stabilizing the conformation of the GGQ loop, as has also been proposed for RF1 (14). Even so, the structure cannot explain why a mutation to G would result in a 90-fold reduced reaction rate (28).

In the ribosome, the closed form of RF2 would clash with P-site tRNA and H69, which is consistent with the observation that *E. coli* RF1 is primarily in the open form in solution (31). Although *Thermus* RF2 is mainly in the closed form at 20°C, thermodynamic data suggested that it too exists predominantly in the open form at the physiological temperature of 75°C (15). Thus, it is unlikely that RF2 binds in the closed form to the ribosome and switches into the open form as a result of codon recognition. More likely, the open form is conformationally variable, and codon recognition imposes restraints on domain 3 that place the GGQ motif in the correct position at the PTC. As also noted for RF1 (14), local rearrangements of specific regions of RF2 are induced by ribosome binding (Fig. 1C).

Helix 69 of the 50S subunit is in a different orientation relative to the structure, with a partially ordered tRNA in the A site (fig. S2) (12). Upon stop-codon recognition, A1913 of this helix stacks onto A1493 (Fig. 2A and fig. S2), thus establishing a connection between the decoding center and the 50S subunit. Also, Q121 of RF2 can make hydrogen bonds with both the 2'-OH of C1914 and the phosphate backbone of U1915. This is consistent with previous biochemical data that shows that the pseudouridylation (32) or deletion (33) of H69 can affect translation termination. A similar change was also seen with RF1 (14), although the details of the A1913/A1493 stack appear different.

The high-resolution structure of RF2 bound to the ribosome with its UGA stop codon provides a structural basis for understanding its role in translational termination. Together with the recently published structure of the RF1-ribosome complex (14), these structures represent a major advance in understanding both stop-codon recognition and peptide release. Stop-codon recognition appears to have many components, and the remaining factor-codon combinations, along with mutagenesis studies, will help clarify additional elements of recognition. We have proposed a model for catalysis that is consistent with the structure and biochemical data. However, both this and the RF1 structure represent the state after hydrolysis and peptide release, with a deacylated tRNA in the P site. Structures of substrate analog complexes at a resolution at which ordered water molecules would be visible, along with more di-

rected biochemical experiments, will therefore be essential for understanding catalysis by these factors.

References and Notes

- M. R. Capecchi, *Proc. Natl. Acad. Sci. U.S.A.* **58**, 1144 (1967).
- E. M. Youngman, M. E. McDonald, R. Green, *Annu. Rev. Microbiol.* **62**, 353 (2008).
- Single-letter abbreviations for the amino acid residues are as follows: A, Ala; C, Cys; D, Asp; E, Glu; F, Phe; G, Gly; H, His; I, Ile; K, Lys; L, Leu; M, Met; N, Asn; P, Pro; Q, Gln; R, Arg; S, Ser; T, Thr; V, Val; W, Trp; and Y, Tyr.
- L. Y. Frolova *et al.*, *RNA* **5**, 1014 (1999).
- K. Ito, M. Uno, Y. Nakamura, *Nature* **403**, 680 (2000).
- K. S. Wilson, K. Ito, H. F. Noller, Y. Nakamura, *Nat. Struct. Biol.* **7**, 866 (2000).
- H. Song *et al.*, *Cell* **100**, 311 (2000).
- B. Vestergaard *et al.*, *Mol. Cell* **8**, 1375 (2001).
- U. B. Rawat *et al.*, *Nature* **421**, 87 (2003).
- B. P. Klaholz *et al.*, *Nature* **421**, 90 (2003).
- S. Petry *et al.*, *Cell* **123**, 1255 (2005).
- M. Selmer *et al.*, *Science* **313**, 1935 (2006).
- Materials and methods are available as supporting material on Science Online.
- M. Lauberg *et al.*, *Nature* **454**, 852 (2008).
- G. Zoldak *et al.*, *Nucleic Acids Res.* **35**, 1343 (2007).
- J. M. Ogle *et al.*, *Science* **292**, 897 (2001).
- J. M. Ogle, F. V. Murphy, M. J. Tarry, V. Ramakrishnan, *Cell* **111**, 721 (2002).
- E. M. Youngman, S. L. He, L. J. Nikstad, R. Green, *Mol. Cell* **28**, 533 (2007).
- D. V. Freistoffer, M. Kwiatkowski, R. H. Buckingham, M. Ehrenberg, *Proc. Natl. Acad. Sci. U.S.A.* **97**, 2046 (2000).
- K. Ito, M. Uno, Y. Nakamura, *Proc. Natl. Acad. Sci. U.S.A.* **95**, 8165 (1998).
- J. M. Ogle, V. Ramakrishnan, *Annu. Rev. Biochem.* **74**, 129 (2005).
- A. V. Zavialov, L. Mora, R. H. Buckingham, M. Ehrenberg, *Mol. Cell* **10**, 789 (2002).
- J. J. Shaw, R. Green, *Mol. Cell* **28**, 458 (2007).
- T. M. Schmeing, K. S. Huang, S. A. Strobel, T. A. Steitz, *Nature* **438**, 520 (2005).
- L. Mora *et al.*, *Mol. Microbiol.* **47**, 267 (2003).
- S. Trobro, J. Aqvist, *Mol. Cell* **27**, 758 (2007).
- V. Dincbas-Renqvist *et al.*, *EMBO J.* **19**, 6900 (2000).
- E. M. Youngman, J. L. Brunelle, A. B. Kochaniak, R. Green, *Cell* **117**, 589 (2004).
- J. L. Brunelle, J. J. Shaw, E. M. Youngman, R. Green, *RNA* **14**, 1526 (2008).
- M. Amort *et al.*, *Nucleic Acids Res.* **35**, 5130 (2007).
- B. Vestergaard *et al.*, *Mol. Cell* **20**, 929 (2005).
- M. Ejby, M. A. Sorensen, S. Pedersen, *Proc. Natl. Acad. Sci. U.S.A.* **104**, 19410 (2007).
- I. K. Ali, L. Lancaster, J. Feinberg, S. Joseph, H. F. Noller, *Mol. Cell* **23**, 865 (2006).
- We thank M. Schmeing for his useful comments and M. Fuchs and C. Schulze-Briese for their help and advice with data collection at the Swiss Light Source. This work was supported by MRC UK, a program grant from the Wellcome Trust, and awards from the Agouron Institute and Louis-Jeanet Foundation. C.N. is supported by a Boehringer-Ingelheim fellowship and R.M.V. is supported by a Gates-Cambridge fellowship. Coordinates for the structure have been deposited in the Protein Data Bank with accession codes 2j15 to 2j18. V.R. holds stock options in Rib-X Pharmaceuticals, a company that develops antibacterial drugs that target the ribosome.

Supporting Online Material

www.sciencemag.org/cgi/content/full/322/5903/953/DC1
Materials and Methods
Figs. S1 and S2
Table S1
References

19 August 2008; accepted 26 September 2008
10.1126/science.1164840

Supporting Online Material for

Insights into translational termination from the structure of RF2 bound to the ribosome

Albert Weixlbaumer*, Hong Jin*, Cajetan Neubauer, Rebecca M. Voorhees, Sabine Petry[§], Ann C. Kelley and V. Ramakrishnan[†]

MRC Laboratory of Molecular Biology
Hills Road
Cambridge CB2 0QH
United Kingdom

*These two authors contributed equally to the work.

[§]Present address: Dept. of Cellular and Molecular Pharmacology, University of California, San Francisco, 600-16th Street, San Francisco CA 94158, USA.

[†]Corresponding author

E-mail: ramak@mrc-lmb.cam.ac.uk

Phone: +44 1223 402213

This PDF files includes:

Materials and Methods

Figures S1 and S2

Table S1

References

Materials and methods

Purification of 70S ribosomes, tRNA, RF2 and mRNA

Thermus thermophilus ribosomes and *E. coli* tRNA^{Phe} were purified as described previously (S1). His-tagged *T. thermophilus* RF2 was overexpressed in *E. coli* and purified as described previously (S2), and the His tag cleaved off using TEV protease. The cleaved tag, any remaining tagged RF2 and the TEV protease itself, were removed by passing the mixture through a Ni-NTA column. Mass spectrometry showed that only a small fraction of Q240 (<5-10%) was methylated. The mRNA used was chemically synthesized by Dharmacon and had the sequence 5' GGC AAG GAG GAG AAU AAA UUC UGA UAC A 3' which contained a UUC Phe codon in the P site (bold) and an RF2-specific UGA stop codon in the A site (underlined bold).

Crystallization of complexes

Complexes of RF2 with the ribosome containing tRNA^{Phe} and mRNA with a UGA codon in the A site were crystallized as described previously for the ribosome-tRNA complex (S1). All complexes were formed in buffer G (5 mM HEPES pH 7.5, 10 mM MgAc, 50 mM KCl, 10 mM NH₄Cl, 6 mM 2-mercaptoethanol). To form an RF2 complex, 70S ribosomes at a final concentration of 4.4 μM were incubated with a 2-fold excess of mRNA and a 4-fold excess of tRNA^{Phe} at 55°C for 30 min, before being further incubated with a 4-fold excess of RF2 for 30 min. The complex was left at room temperature for 30 min prior to crystallization. Crystals were grown in sitting drop vapor diffusion experiments in which 2.4 μl of ribosomal complex including 2.8 mM Deoxy Big Chap (Hampton Research, added directly before setup) was mixed with 2 μl reservoir solution containing 0.1M KCl, 0.1M Tris-HAc pH7, 3-4.5%(w/v) PEG20K, 3-4.5%(w/v) PEG550MME and left to equilibrate at 20°C. Crystals grew in 2-3 weeks to the size of up to 50x70x700 μm. The crystals were sequentially transferred to cryo-protecting solution (0.1 M KCl, 10 mM NH₄Cl, 10 mM MgAc, 0.1M Tris-HAc pH 7, 5% PEG 20K, 25% PEG550MME), and frozen by plunging into liquid nitrogen. All data collection was carried out at 100K.

Data collection, refinement and model-building

X-ray diffraction data were collected from five separate regions of a single crystal at beamline X10SA at the Swiss Light Source, Villigen. Data were integrated and scaled with the XDS package (*S3*). A starting model consisting of our previous high-resolution structure of the 70S ribosome (*S1*) with all its ligands omitted was used for refinement. Prior to its use in refinement, errors in the sarcin-ricin loop, a stem-loop of the L1 binding region of 23S RNA and in protein L28 were corrected. Refinement was carried out using CNS (*S4*) as described previously (*S1*) or using the program Phenix (*S5*) as follows: Initially, rigid body refinement of each of the two 70S molecules was done, followed by position and B-factor refinement. With Phenix, an additional step of TLS refinement was done after B-factor refinement, in which the TLS groups defined were the head, 5' domain, platform and 3' minor domain of the 30S subunit; the body and L1 stalk of the 50S subunit, and 5S RNA. The initial R/R_{free} of the model was 27.2/32.0. Sigma A weighted difference Fourier maps clearly showed the presence of the mRNA, tRNA and RF2 ligands. Initially P-site tRNA and codon were built in and the model re-refined. Using the high resolution *E. coli* structure (*S6*), a homology model for ribosomal protein L11 and the L11 binding region of 23S RNA was derived and built into the density. Then E-site tRNA, the domains of RF2 and the A-site codon were placed, but key regions such as the SPF loop, the GGQ loop, residues A1492, A1493 and G530 in the decoding center and the less well-ordered domain 1 of RF2 were left out, and a new round of refinement as above, was carried out. Finally, the missing regions were built in. The final model included RF2 residues 6-356, the entire E- and P-site tRNA^{Phe}, the A- and P-site codons and two bases of the E-site codon. The maps shown in all figures are derived from CNS.

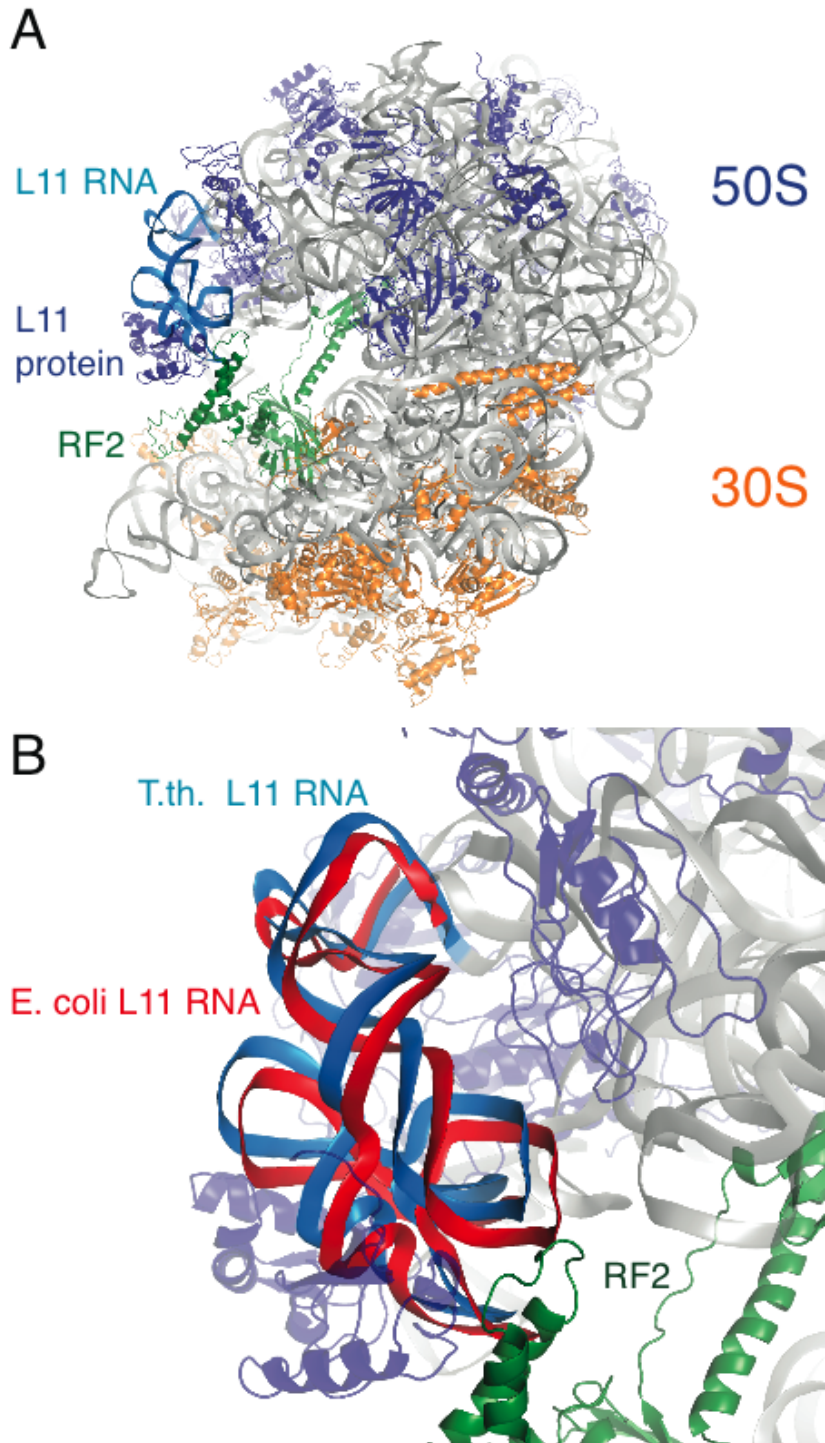


Figure S1. Interaction of Domain 1 of RF2 with the L11 region of the ribosome.
 A. Overview showing the interaction of Domain 1 of RF2 (green) with the L11-RNA region of the 50S subunit. B. Details showing the changes in the conformation of the L11-RNA region in the RF2-bound form (blue) with its conformation in the empty *E. coli* ribosome (red, from ref. *S6*). Domain 1 of RF2 consists of a bundle of 4 helices,

including an additional N-terminal helix not present in RF1. Although this region is poorly ordered the helices of RF2 are visible in maps calculated to 4-6Å resolution, allowing the domain to be placed as a rigid body. As seen in previous low-resolution studies (*S2, S7, S8*), Domain 1 interacts with the L11 region of the ribosome. This interaction is made possible by movements of both Domain 1 relative to the isolated RF2 crystal structure (*S9*) (Fig. 1C) and of the L11/RNA region relative to the structure of an empty ribosome (*S6*). As a result, the L11-RNA complex and, to a lesser extent, protein L10 were better ordered than in the high-resolution 70S structure in the absence of RF2 (*S1*). There is no evidence for a change in conformation of the N-terminal domain of L11 relative to the rest of the protein or its RNA region as suggested by earlier low-resolution studies (*S2*). Differences in interaction with this region between RF1 and RF2 may be functionally important. For example, deletion of L11 preferentially reduces RF1 function (*S10*) whereas mutations in the L11-binding RNA region affected only RF2 function (*S11*). However, a recent study showed that mutations in both domains of L11 affected both factors equally (*S12*).

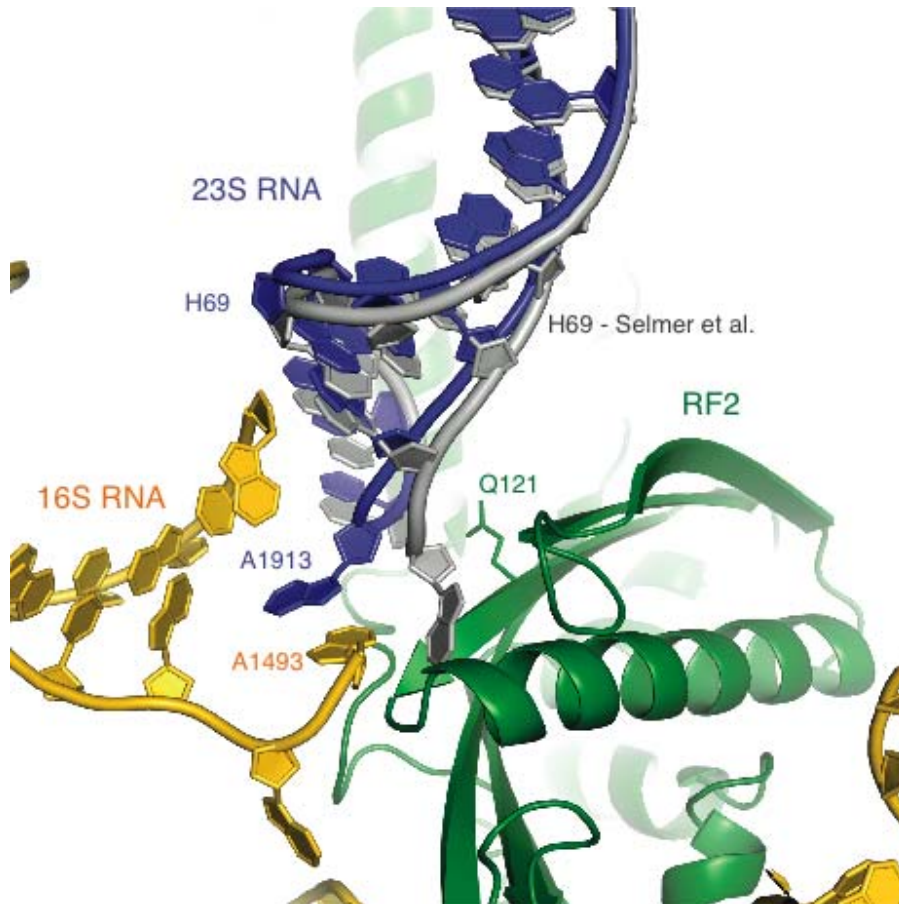


Figure S2. Changes in the conformation of helix 69 of 23S RNA (blue) relative to its conformation in a ribosome with a tRNA in the A site (gray, from ref. *SI*).

Table S1. Summary of crystallographic data and refinement

70S – RF2 complex	
Data collection	
Space Group	P2 ₁ 2 ₁ 2 ₁
Cell dimensions	
<i>a</i> , <i>b</i> , <i>c</i> (Å)	<i>a</i> =211.3 <i>b</i> =450.9, <i>c</i> =614.0
α , β , γ (°)	α = β = γ =90
Resolution (Å)	50-3.45 (3.5-3.45)*
<i>R</i> _{sym}	17.5 (83.1)
<i>I</i> / σ <i>I</i>	8.19 (1.74)
Completeness (%)	99.6 (99.5)
Redundancy	5.46 (3.63)
Refinement	
Resolution (Å)	50.0-3.45
No. unique reflections	759,980
<i>R</i> _{work} / <i>R</i> _{free}	21.3/26.2 (19.2/24.3)**
No. atoms	
RNA	99689 (per molecule)
Protein	50328 (per molecule)
Ions	549 (per molecule)
<i>B</i> -factors	
RNA	82.5
Protein	99.8
Ions	54.7
R.m.s. deviations	
Bond lengths (Å)	0.007 (0.007)**
Bond angles (°)	1.2 (1.6)**

* *I* / σ *I* = 2.33 at 3.5 Å.

**Values in parenthesis represent refinement results when using phenix and multiple TLS groups

References

- S1. M. Selmer *et al.*, *Science* **313**, 1935 (2006).
- S2. S. Petry *et al.*, *Cell* **123**, 1255 (2005).
- S3. W. Kabsch, *J. Appl. Cryst.* **26**, 795 (1993).
- S4. A. T. Brünger *et al.*, *Acta Crystallogr D Biol Crystallogr* **54**, 905 (1998).
- S5. P. V. Afonine, R. W. Grosse-Kunstleve, P. D. Adams, *CCP4 Newsl.* **42**, contribution 8. (2004).
- S6. B. S. Schuwirth *et al.*, *Science* **310**, 827 (2005).
- S7. U. B. Rawat *et al.*, *Nature* **421**, 87 (2003).
- S8. B. P. Klaholz *et al.*, *Nature* **421**, 90 (2003).
- S9. G. Zoldak *et al.*, *Nucleic Acids Res* **35**, 1343 (2007).
- S10. W. Tate, H. Schulze, K. Nierhaus, *J. Biol. Chem.* **258**, 12816 (1983).
- S11. A. L. Arkov, D. V. Freistroffer, M. Ehrenberg, E. J. Murgola, *Embo J* **17**, 1507 (1998).
- S12. H. Sato, K. Ito, Y. Nakamura, *Mol Microbiol* **60**, 108 (2006).